Electronic Supplementary Material (ESI) for Journal of Materials Chemistry C.
This journal is © The Royal Society of Chemistry 2017

Electronic Supplementary Information

Poly(*N*-isopropylacrylamide) Capped Plasmonic Nanoparticles as Resonance Intensity-based Temperature Sensors with Linear Correlation

Yiyi Liu‡[ae], Xiaohui Dai‡[d], Sudaraka Mallawaarachchi[b], Harini Hapuarachchi[b], Qianqian Shi[ae], Dashen Dong[ae], San H. Thang[c], Malin Premaratne[b] and Wenlong Cheng*[ae]

[a]Department of Chemical Engineering, Monash University, Clayton, Victoria 3800, Australia

[b]Advanced Computing and Simulation Laboratory (AχL), Department of Electrical and Computer Systems Engineering, Faculty of Engineering, Monash University, Clayton, Victoria 3800, Australia

[c]School of Chemistry, Monash University, Clayton, Victoria 3800, Australia

[d]Institute of Green Chemistry and Chemical Technology, Jiangsu University, Zhenjiang 212013, China

[e]The Melbourne Centre for Nanofabrication, Clayton, Victoria 3800, Australia

*Address correspondence to wenlong.cheng@monash.edu

Including: Experimental section, mathematical modelling and supporting figures.

Experimental Section

Materials. Gold(III) chloride trihydrate ($HAuCl_4 \cdot 3H_2O$, ≥99.9%), sodium borohydride ($NaBH_4$), trisodium citrate, hexadecyltrimethylammonium bromide (CTAB), silver nitrate ($AgNO_3$), L-ascorbic acid, cetyltrimethylammonium chloride solution (CTAC, 25 wt% in H_2O), *N*-isopropylacrylamide (NIPAM, ≥99.9%), benzyl benzodithioate (96%), *n*-butylamine (99.5%) and chloroform-d were purchased from Sigma-Aldrich. 2,2'-Azobis(isobutyronitrile) (AIBN) was purchased from Polysciences Inc. Hydrochloric acid (HCl, 32 wt%) was purchased from AJAX. Ammonium hydroxide ($NH_3•H_2O$, 25 wt%) was from Chem Supply. Hydrogen peroxide (H_2O_2, 30 wt%), *n*-hexane, 1,4-dioxane, methanol, tetrahydrofuran (THF) and diethyl ether were obtained from Merck KGaA. All chemicals were used as received unless otherwise indicated. Demineralized water was used in all aqueous solutions, which were further purified with a Milli-Q system (Millipore). All glassware used in the gold nanoparticles synthesis procedures was cleaned in a bath of freshly prepared aqua regia and was rinsed thoroughly in H_2O prior to use. Gilder extrafine bar grids (2000 mesh with 7×7 μm^2 square holes) were purchased from Ted Pella.

Synthesis of Gold Nanospheres (AuNSs). Gold nanospheres was synthesized according to our previously published procedures.[1] Typically, 2 mL $HAuCl_4$ solution (25 mM) was added into 170 mL Milli-Q water and heated until boiling, followed by the addition of 6 mL sodium citrate solution (34 mM) into the above solution while stirring vigorously. The solution turned wine-red after 3 minutes heating, which was the sign of the formation of AuNSs. A further 10 minutes' boiling of the above solution was maintained before the heat source was removed, and the dispersion was cooled down to room temperature. The NS solution was then stored in the refrigerator for further use.

Synthesis of Gold Nanorods (AuNRs). Gold nanorods was prepared through seed-mediated method as described in our previous paper.[2] At first, a seed solution was prepared. CTAB (5.0 mL, 0.2 M) and $HAuCl_4$ (5.0 mL, 0.5 mM) was mixed together at 30°C with gently stirring, followed by the addition of ice-cold $NaBH_4$ (0.6 mL, 0.01 M) solution into the mixture and a 10 second period of vigorous stirring was given. The solution changed into a brownish-yellow color immediately after the addition of $NaBH_4$ and was then aged at 30°C prior to use.

Growth solution was prepared by mixing CTAB (15.0 mL, 0.2 M) and $AgNO_3$ solution (4 mM, 0.6 mL) together, and then $HAuCl_4$ (15.0 mL, 1.0 mM) and ascorbic acid (240 µL, 80 mM) were added. Each time after adding a new reactant, the solution was shaken once to ensure satisfactory mixing. The mixture changed from a yellowish color to colorless upon the mixing well of ascorbic acid. To grow CTAB-capped AuNRs, 36 μL of premade seed was added into the growth solution and mixed well. The whole mixture was then aged at 30°C for two hours. Upon finishing the growth cycle, the AuNRs solution was centrifuged out at 7000 rpm for 10 minutes, and the supernatant was removed and AuNRs residue was re-dispersed in water, placing in the refrigerator for further use.

Synthesis of Gold Nanobipyramids (AuNBPs). AuNBPs were prepared using the typical seed mediated method described in our previous paper.[3] At first, gold seeds solution was prepared by reducing $HAuCl_4$ with $NaBH_4$ in the presence of trisodium citrate. Freshly prepared $NaBH_4$ solution (1.0 mL of 100 mM) was added into a 40mL solution comprising $HAuCl_4$ (0.25 mM) and trisodium citrate (0.25 mM) under vigorous stirring, and then the orange-red solution was aged at room temperature for at least two hours before use.

Then a growth solution was prepared by mixing $HAuCl_4$ (2 mL, 25 mM), CTAB (98 mL, 0.1 M), $AgNO_3$ (1 mL, 10 mM), HCl (2 mL, 1.0 M) and L-ascorbic acid (0.8 mL, 0.1 M), followed by the addition of 0.4 mL of the prepared seeds. Each time after adding a new reactant, the solution was shaken once to ensure satisfactory mixing. Then the solution was left undisturbed and aged at 30°C in a water bath overnight.

To obtain high purity AuNBPs, a three-step purification method was utilized after the preparation of AuNBPs solution.[4] Firstly, the as-grown AuNBPs sample (100 mL) was centrifuged at 7830 rpm for 30 minutes, and the AuNBPs residue was re-dispersed in a CTAC solution (80 mM, 75 mL). Then, $AgNO_3$ (0.01 M, 36 mL) and ascorbic acid (0.1 M, 18 mL) were added into the mixture and mixed well. The resultant solution was kept in a water bath at 65°C for 4 hours, during which Ag was overgrown on the Au nanocrystals to produce Au@Ag nanorods. The Au@Ag nanorods were then centrifuged at 6000 rpm for 10 minutes and the Au@Ag nanorods residue was re-dispersed in CTAB (50 mM, 60 mL) and left undisturbed for

2 hours at room temperature. During this process, the Au@Ag nanorods aggregated and formed precipitates at the bottom and the sphere-like nanoparticles remained in the supernatant, which was later discarded. This step was repeated twice to ensure the fully removal of the sphere-like nanoparticles. The Au@Ag nanorods precipitates were then re-dispersed in CTAB (50 mM, 50 mL) and the solution was mixed gently with $NH_3 \cdot H_2O$ (30 wt%, 1.4 mL) and H_2O_2 (30 wt%, 0.7 mL) and kept undisturbed at room temperature for 2 hrs. The Ag segments were etched away and the AgCl precipitates were formed. The clear supernatant was then carefully taken out and centrifuged at 10000 rpm for 15 minutes, and the obtained pure AuNBPs were re-dispersed in a CTAB solution (50 mM, 25 mL) for further use.

Synthesis of PNIPAM. PNIPAM was synthesized using a modified RAFT polymerization technique as per litearture.[5, 6] Before polymerization, monomer *N*-isopropylacrylamide was recrystallized in *n*-hexane (in a ratio of 1 g: 5 mL). Benzyl benzodithioate (10 μL, 4.84×10^{-5} mol), AIBN (1.63 mg, 1×10^{-5} mol) and *N*-isopropylacrylamide (2.5 g, 0.022 mol) were put into a round bottom flask, followed by the addition of 6 mL of 1,4-Dioxane. Then three vacuum-freeze-thaw cycles were conducted and the flask was immersed into an oil bath at 70°C with stirring. After 24 hours, the flask was cooled to room temperature and the product was precipitated in *n*-hexane and dried out. Then the polymer was dissolved in 5 mL of THF and precipitated in 50 mL of diethyl ether. After repeating the dissolving-precipitation procedure for three times, the obtained pink PNIPAM (conversion: 60%) was dried in a vacuum oven at 35°C for at least 24 hours.

$M_{n,GPC}$ = 32060 g/mol, M_w/M_n = 1.29, $M_{n,NMR}$ = 34000. ^{1}H NMR δ_H ($CDCl_3$, ppm): 4.00 (N-C**H**), 1.46~2.34 (N-(O=C)-C**H**-C**H**$_2$), 1.14 (N-CH(C**H**$_3$)$_2$).

Synthesis of SH-PNIPAM. SH-PNIPAM was synthesized according to literature with slight modifications.[7] To obtain the thiol-terminated PNIPAM, the dithioester ended PNIPAM was reduced by *n*-butylamine in THF. 1.0 g of dithioester ended PNIPAM was dissolved in 5 mL

THF and an excess amount of *n*-butylamine (50 times, 0.15 mL) was added under the protection of N_2. A quick color change of the solution from pink to pale yellow was observed, which indicated the reduction of dithioester ended PNIPAM to form SH-PNIPAM. The mixture was stirred for 2 hours to ensure the completion of the reduction and then precipitated out in diethyl ether. After repeating the dissolving-precipitation procedure twice, the obtained white product was dried in a vacuum oven for at least 24 hours. From the UV-Vis spectra, the dithioester peak at 310 nm disappeared after the reduction, which confirmed the formation of thiol.

Preparation of SH-PNIPAM Protected Au Nanoparticles. SH-PNIPAM protected Au nanoparticles were prepared using procedures described in literature with slight modifications.[8] The general method presented here is suitable for all the three morphologies of gold nanoparticles (NSs, NRs and NBPs).

40 mg SH-PNIPAM was weighted out and dissolved into 2 mL water at room temperature. The solution was gently stirred to aid the SH-PNIPAM dissolving process. 20 mL of the NSs solution was centrifuged and the supernatant was discarded. Then, the residue was added into the SH-PNIPAM/water solution and the mixture was stirred at 500 rpm for 24 hours. After the completion of the ligand exchange process, 4 mL of methanol was added into the solution and the mixture was centrifuged at 12100 rpm for 30 minutes. Three further methanol washing cycles were concluded prior to placing the SH-PNIPAM protected gold NSs in a vacuum oven. The solution was dried for 24 hours while maintaining a temperature of 30 °C. The resultant NS@PNIPAM was re-dissolved in 2 mL of water and stored in the refrigerator for further use.

Preparation of the Standard Sample for UV Measurements. The standard sample of NS@PNIPAM was prepared by dissolving 0.1 mL of SH-PNIPAM protected NSs in 2.9 mL of water, with NSs concentration calculated to be ~1.178 nM. The NR@PNIPAM standard sample was prepared by dissolving 0.02 mL of SH-PNIPAM protected NRs in 2.98 mL water, with NRs concentration calculated to be ~0.0224 nM. The NBP@PNIPAM standard sample was prepared by dissolving 0.01 mL SH-PNIPAM protected NBPs in 2.99 mL water, with NBPs concentration calculated to be ~0.000857 nM.

For the salted samples, unless specified, the NaCl concentration is 12 mM for all of NS, NR and NBP.

Preparation of Samples for Dynamic Light Scattering (DLS) Measurements. NS@PNIPAM was prepared by dissolving 0.1 mL of SH-PNIPAM modified NS in 2.9 mL water. After mixing well, 1 mL of this solution was acquired as the sample for DLS measurements.

Instrumentation. The morphologies of Au NS@PNIPAM, Au NR@PNIPAM and Au NBP@PNIPAM were obtained through TEM (FEI Tecnai G2 T20 TWIN LaB6 TEM operating at 200 kV). Temperature controlled UV measurements were taken using an Agilent Cary 100 UV-Vis spectrophotometer with a circulating water pump, and samples were equilibrated at each temperature (each sample was measured at temperatures: 25, 30, 32, 34, 36, 38, 40, 42, 44, 46, 48 and 50 °C) for at least 3 minutes before measuring the absorption spectra. The NMR spectrum was measured using a Bruker Advance III 400 (9.4 Tesla magnet) with a 5 mm broadband auto-tunable probe with Z-gradients and BACS 60 tube autosampler. GPC was performed on a system comprising a Shimadzu LC-20AD pump and a Shimadzu RID-20A refractive index detector equipped with 4 × Shodex columns (K-805, K-805, K-805, K-801 each 300 mm × 8 mm providing an effective molecular weight range of 3,000-100,000). The eluent was tetrahydrofuran (THF) at 40°C (flow rate: 1 mL min^{-1}). Number average (M_n) and weight average (M_w) molecular weights were evaluated using the software package: Shimadzu. The GPC columns were calibrated with low dispersity poly(methyl methacrylate) (Shodex) ranging from 3,100 to 105,000 g mol^{-1} and molecular weights were reported as poly(methyl methacrylate) equivalents. A third order polynomial was used to fit the log(Mp) against the time calibration curve, which appeared approximately linear across the molecular weight range from 2×10^2 to 2×10^6 g mol^{-1}. Dynamic light scattering (DLS) measurements were carried out on a Malvern Zetasizer Nano ZS (laser wavelength of 633 nm, fixed scattering angle of 173°, measured at temperatures: 25, 30, 31, 32, 33, 34, 35, 36, 38, 40, 42, 44, 46, 48 and 50 °C). At each temperature, the sample was equilibrated for 120 seconds and measured thrice, using which the mean value of the size (main peak value of the size distribution by intensity curves) was recorded.

Mathematical modelling

A mathematical model, based on Mie theory was rigorously and numerically analyzed to establish a theoretical foundation for the optical characteristics of a PNIPAM capped AuNRs solution engulfed in a water medium. For simplicity, the engulfing medium was assumed to comprise the external water medium as well as the PNIPAM layer surrounding each AuNR. Due to the presence of chemical interface damping and the known absorptive characteristics of the combined medium, it was assumed that the medium maintains a complex permittivity denoted by ϵ_m within the studied wavelengths. This approach enables the medium permittivity to capture both temperature (T) and wavelength (λ) dependencies observed experimentally. The engulfed AuNRs were assumed to be randomly oriented and morphologically analogous to elongated ellipsoids. Furthermore, effects such as thermal expansion, morphological distortions caused due to maintaining AuNRs at a certain temperature for prolonged durations[9] and collective atomic and thermal effects[10] are assumed to be negligible and therefore ignored in the model.

We use the extinction coefficient (γ) as a measure of the level of absorbance in our model. Although the extinction coefficient generally takes both absorption and scattering into account, for particles with negligible dimensions compared to incident wavelengths, absorbance dominates over scattering. Thus, absorbance spectra are typically observed when extinction spectra are measured experimentally.[11]

The extinction coefficient of a model of this nature is well approximated using the Gans' extinction coefficient, which is based on the dipole approximation and derived as an extension to Mie theory, expressed by[11, 12]:

$$\gamma = \frac{2\pi N V \epsilon_m^{3/2}}{3\lambda} \sum_{j=\{A,B,C\}} \frac{\left(\frac{1}{P_j^2}\right)\epsilon_2}{\left(\epsilon_1 + \frac{1-P_j}{P_j}\epsilon_m\right)^2 + \epsilon_2^2},\#(1)$$

where N denotes the number of particles per unit volume and V denotes the volume of each particle. The term P_j represents the depolarization factors for the three axes of the AuNR, denoted by $j = \{A,B,C\}$, where $A > B = C$, given by:

$$P_A = \frac{1-e^2}{e^2}\left[\frac{1}{2e}\ln\left(\frac{1+e}{1-e}\right) - 1\right],\#(2a)$$

$$P_B = P_C = \frac{1-P_A}{2},\#(2b)$$

where,

$$e = \sqrt{1 - \left(\frac{B}{A}\right)^2}.\#(3)$$

Furthermore, we assumed that the complex dielectric function of gold is described by the Drude-like dielectric function, described by[13]:

$$\epsilon(\omega) = \epsilon_1(\omega) + i\,\epsilon_2(\omega) = \epsilon_{core}(\omega) - \frac{\omega_p^2}{\omega(\omega + i\Gamma)},\#(4)$$

where ω_p is the unscreened plasma frequency of the metal and Γ is the Drude damping rate. The response of the bound ions and electrons that account for effects such as inter-band transitions is denoted by $\epsilon_{core}(\omega)$.

Let λ_{max} denote the wavelength at which the Longitudinal Surface Plasmon Resonance (LSPR) peak occurs and γ_{max} denote the relevant absorbance value at λ_{max}. The real and imaginary parts of the Drude-like formula at λ_{max} take the form,

$$\epsilon_1(\omega) = \epsilon_{core}(\omega) - \frac{\omega_p^2}{\Gamma^2 + \frac{4\,c^2\pi^2}{\lambda_{max}{}^2}}\#(5)$$

$$\epsilon_2(\omega) = \frac{\Gamma\lambda_{max}\,\omega_p^2}{2c\,\pi\left(\Gamma^2 + \frac{4\,c^2\pi^2}{\lambda_{max}{}^2}\right)}\#(6)$$

By substituting the real and imaginary parts for gold permittivity from (5) and (6), and assuming λ_{max} nearly equals the relevant free space wavelength, it is possible to modify (1) to obtain

$$\gamma_{max} = \frac{NV\epsilon_m^{\frac{3}{2}}\Gamma\lambda_{max}^{\ 2}\,\omega_p^2}{3c\sigma_3}\sum_j \frac{\frac{1}{P_j^2}}{\left[\epsilon_{core} + \frac{1-P_j}{P_j}\epsilon_m - \sigma_2\right]^2 + \sigma_1},\#(5)$$

where,

$$\sigma_1 = \frac{\Gamma^2\lambda_{max}^{\ 6}\omega_p^4}{4c^2\pi^2\sigma_3^2},\#(6a)$$

$$\sigma_2 = \frac{\lambda_{max}^{\ 2}\omega_p^2}{\sigma_3},\#(6b)$$

$$\sigma_3 = 4\pi^2c^2 + \Gamma^2\lambda_{max}^{\ 2}.\#(6c)$$

The term P_j represents the depolarization factors for the three axes of the AuNR, denoted by $j = \{A,B,C\}$, where $A > B = C$, given by (2a), (2b) and (2c) and c denotes the speed of light. Based on (5), it is evident that for a given AuNR@PNIPAM solution, to observe a temperature dependent variation for γ_{max}, the medium permittivity ϵ_m must vary with temperature. However, pristine solutions of AuNRs engulfed in water fail to exhibit such a thermal variation.[14] Furthermore, to maintain a linear trend for γ_{max} with temperature, ϵ_m must show a unique and highly specific temperature dependent variation pattern.

Data samples collected during the reheating cycles of the first 10 days for the unsalted, standard sample of AuNR@PNIPAM were used for simulation purposes and the values of the parameters Γ, ω_p and ϵ_{core} are amply available in literature.[15] The simulation line in Figure 2c was obtained using averaged data from the aforementioned 10 days for the temperature measurements of 34 °C and 50 °C only. The standard, purely numerical, Newton-Raphson method was used to solve equation (5) for complex ϵ_m in order to compute data for Figure 2d and Figure S6.[16]

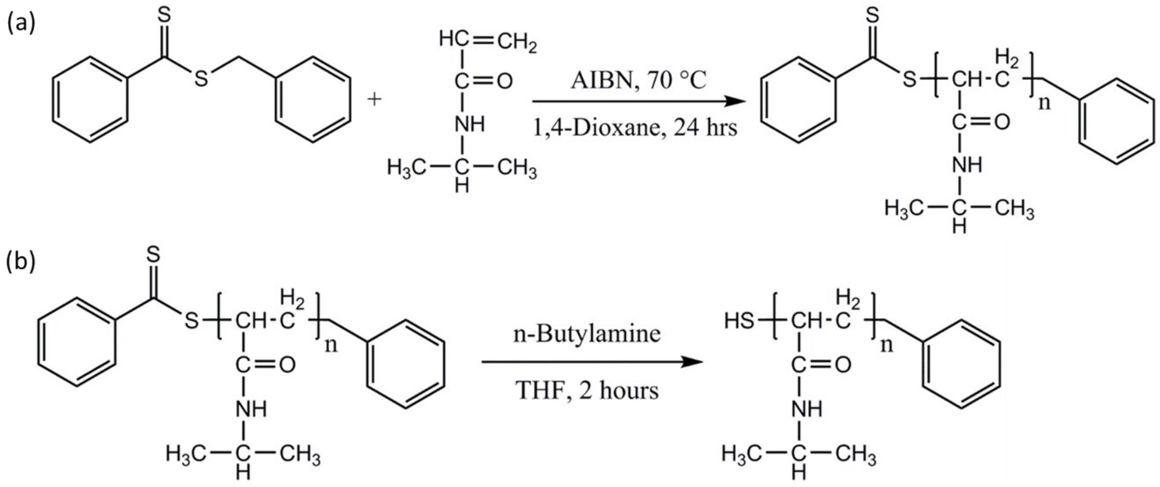

Figure S1. Reaction schemes for (a) RAFT polymerization of NIPAM, (b) Reduction of dithioester terminated PNIPAM into thiol-terminated PNIPAM using *n*-Butylamine.

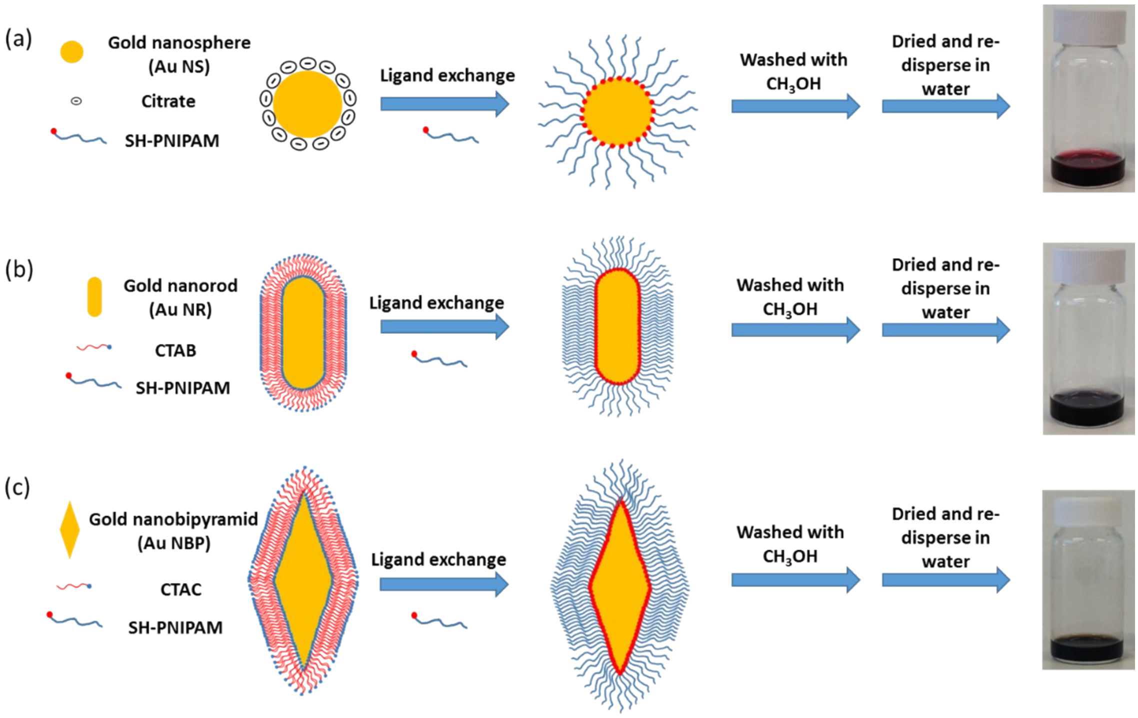

Figure S2. Schemes of preparation of (a) NS@PNIPAM, (b) NR@PNIPAM and (c) NBP@PNIPAM.

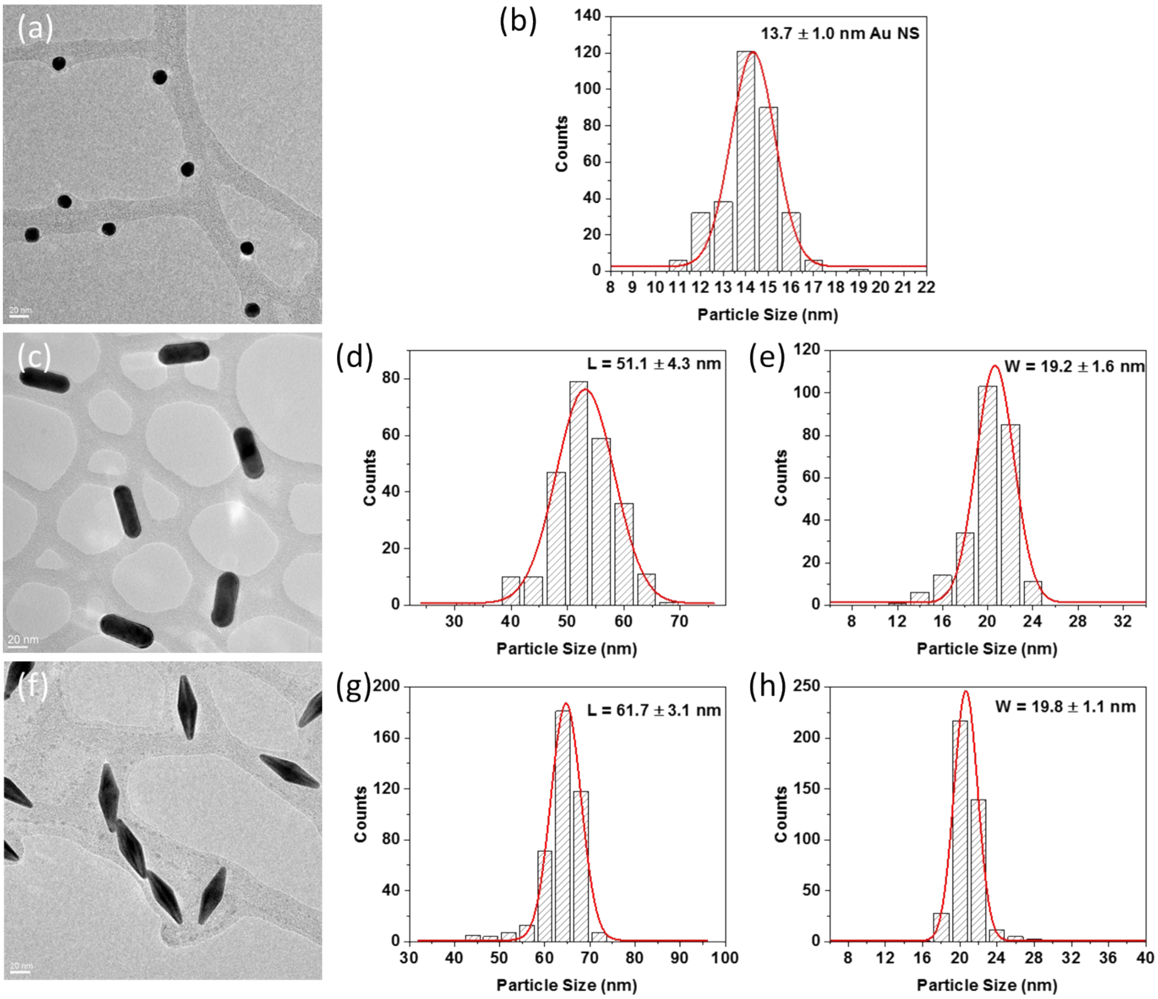

Figure S3. TEM characterizations of (a) NS@PNIPAM, (c) NR@PNIPAM and (f) NBP@PNIPAM, scale bars are 20 nm. (b) is the histogram of NS@PNIPAM gold core sizes from TEM images, the curve represent Gaussian fit of distribution. (d) and (g), (e) and (f) are corresponding histograms of lengths and widths of NR@PNIPAM and NBP@PNIPAM gold cores from TEM images, curves in these plotting are Gaussian fits of distribution.

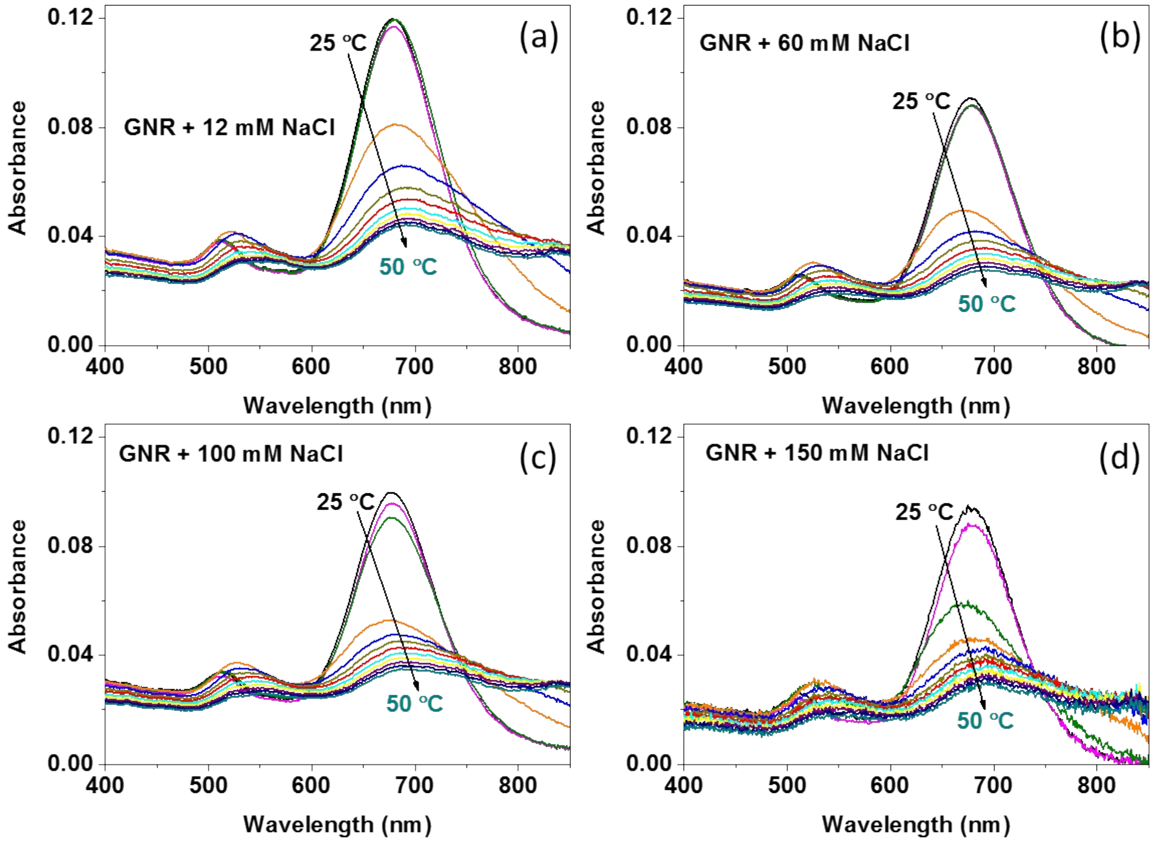

Figure S4. (a) (b) (c) (d) Thermoresponsive behaviours of NR@PNIPAM in aqueous solutions with 12 mM, 60 mM, 100 mM and 150 mM NaCl from 25 to 50 °C.

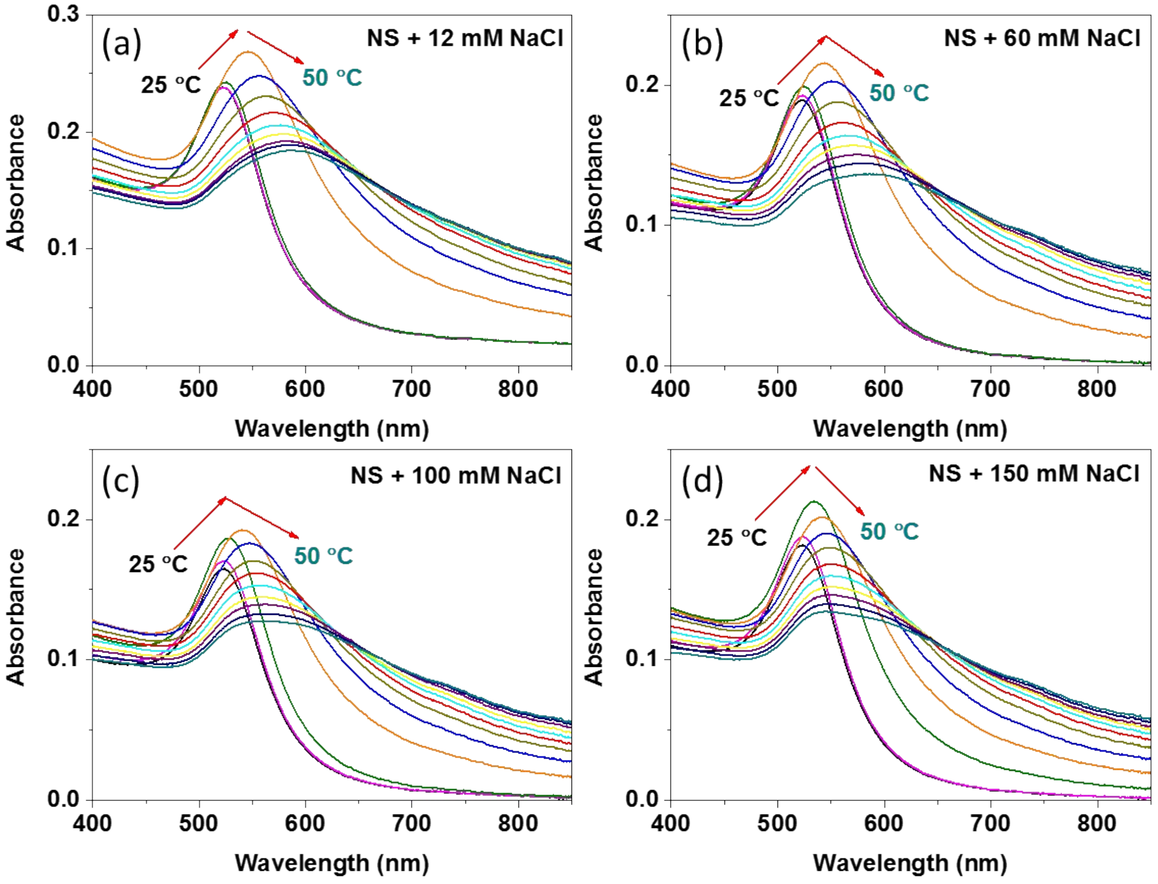

Figure S5. (a) (b) (c) (d) Thermoresponsive behaviours of NS@PNIPAM in aqueous solutions with 12 mM, 60 mM, 100 mM and 150 mM NaCl from 25 to 50 °C.

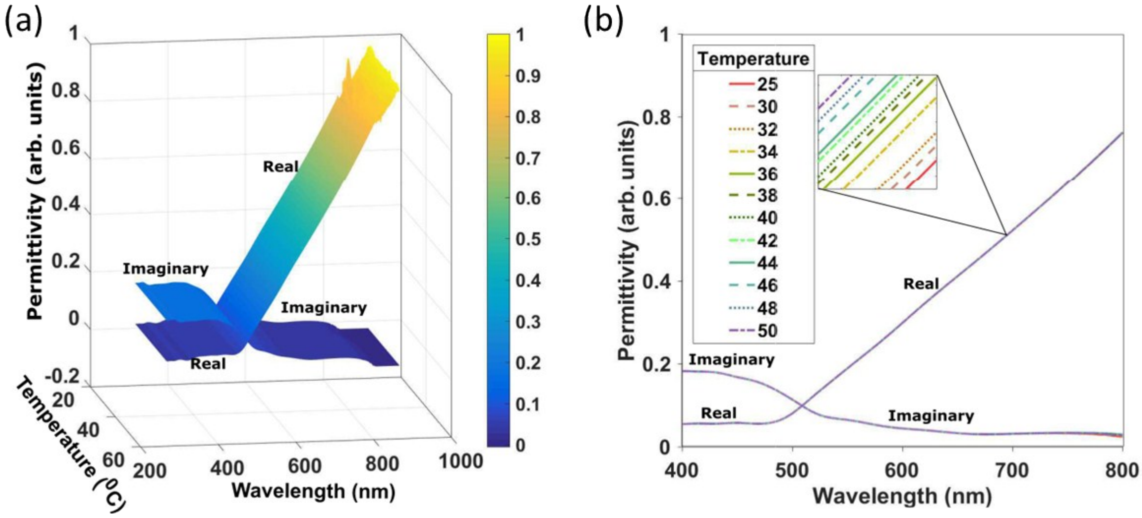

Figure S6. (a) Surface plot of the real and imaginary parts of the normalized medium permittivity (ϵ_m) calculated by numerically solving equation (5) for measured values of γ. (b) Line plots for the same quantities with the insert depicting the splitting pattern around the LSPR peak point.

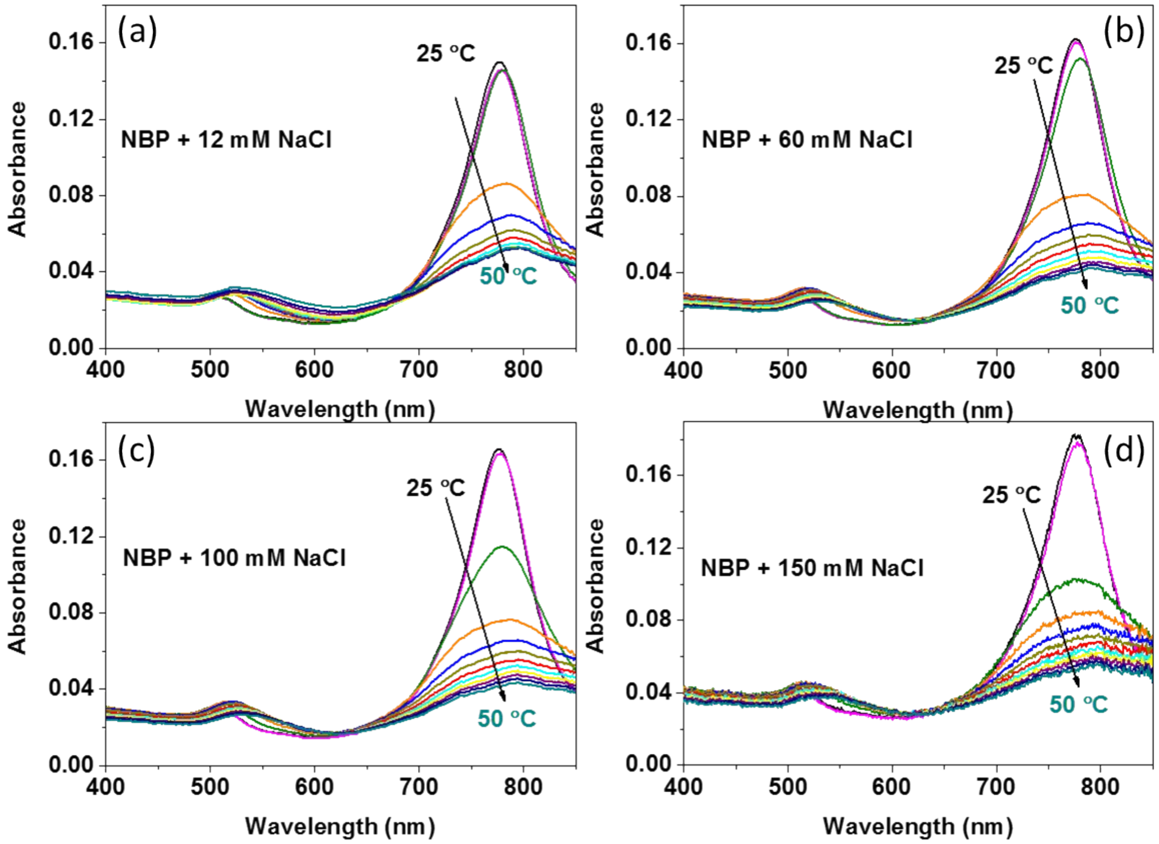

Figure S7. (a) (b) (c) (d) Thermoresponsive behaviours of NBP@PNIPAM in aqueous solutions with 12 mM, 60 mM, 100 mM and 150 mM NaCl from 25 to 50 °C.

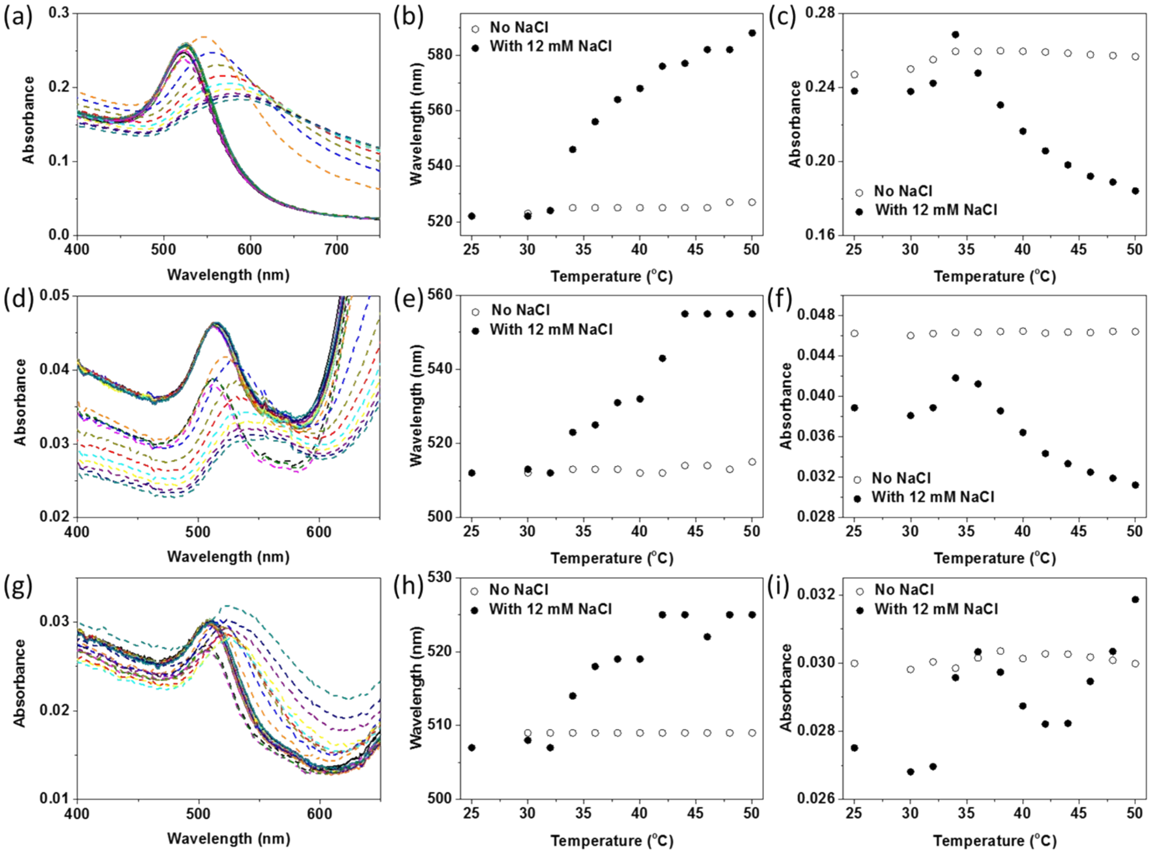

Figure S8. (a) Thermoresponsive behaviour of NS@PNIPAM without (solid line) and with NaCl (dash line) from 25 to 50 °C. (b) and (c) Plotting of wavelengths and peak intensities of NS@PNIPAM to solution temperatures. (d) Thermoresponsive behaviour of transverse mode of NR@PNIPAM without (solid line) and with NaCl (dash line) from 25 to 50 °C. (e) and (f) Plotting of wavelengths and peak intensities of the transverse mode of NR@PNIPAM to solution temperatures. (g) Thermoresponsive behaviour of transverse mode of NBP@PNIPAM without (solid line) and with NaCl (dash line) from 25 to 50 °C. (h) and (i) Plotting of wavelengths and peak intensities of the transverse mode of NBP@PNIPAM to solution temperatures.

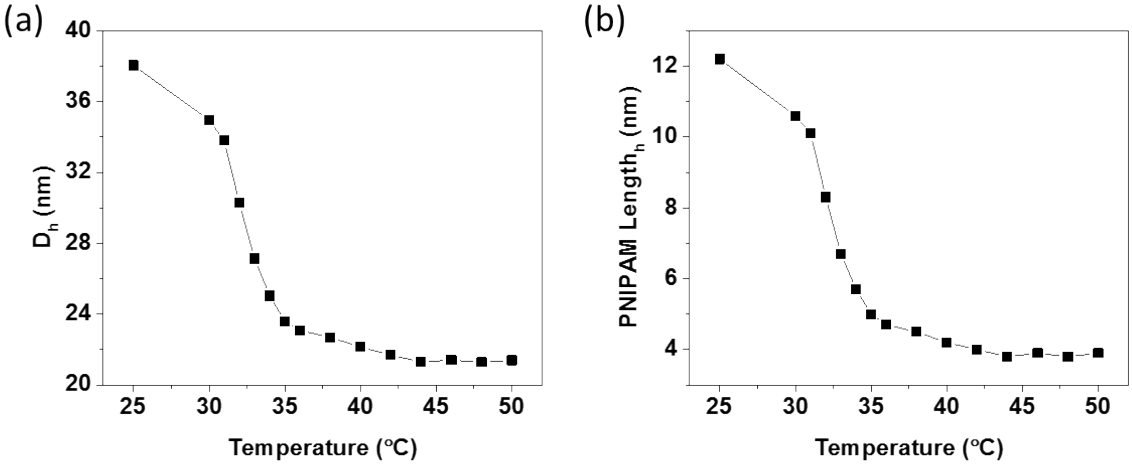

Figure S9. Dynamic light scattering (DLS) data showing (a) the change in hydrodynamic diameters (D_h) of NS@PNIPAM as solution temperature is increased. (b) The change in PNIPAM ligands lengths of NS@PNIPAM as solution temperature is increased.

Repeat Cycles	Hydrodynamic Diameters (D_h) (nm)
Repeat Cycle 1@25 °C	38.9
Repeat Cycle 1@40 °C	100.2
Repeat Cycle 2@25 °C	48.2
Repeat Cycle 2@40 °C	98.7

Table S1. Dynamic light scattering (DLS) data showing the change in hydrodynamic diameters (D_h) of NS@PNIPAM aqueous solution at the presence of 12 mM NaCl when doing cycling test.

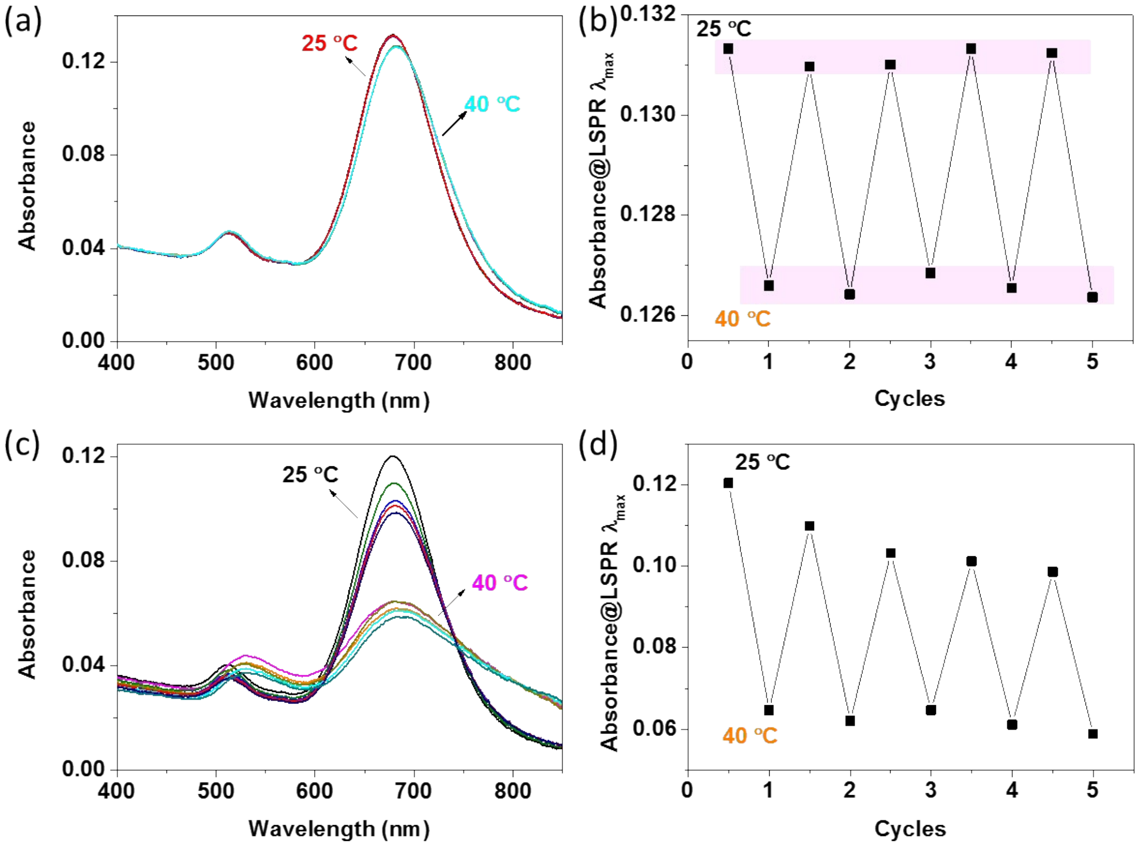

Figure S10. (a) Cycling test of NR@PNIPAM between 25 to 40 °C in aqueous solution without NaCl. (b) Reversibility of the longitudinal mode peak intensity of NR@PNIPAM as a function of the number of heating and cooling cycles in aqueous solution without NaCl. (c) Cycling test of NR@PNIPAM with NaCl in the aqueous solution between 25 to 40 °C. (d) The longitudinal mode peak intensity of NR@PNIPAM with NaCl in the aqueous solution as a function of the number of heating and cooling cycles.

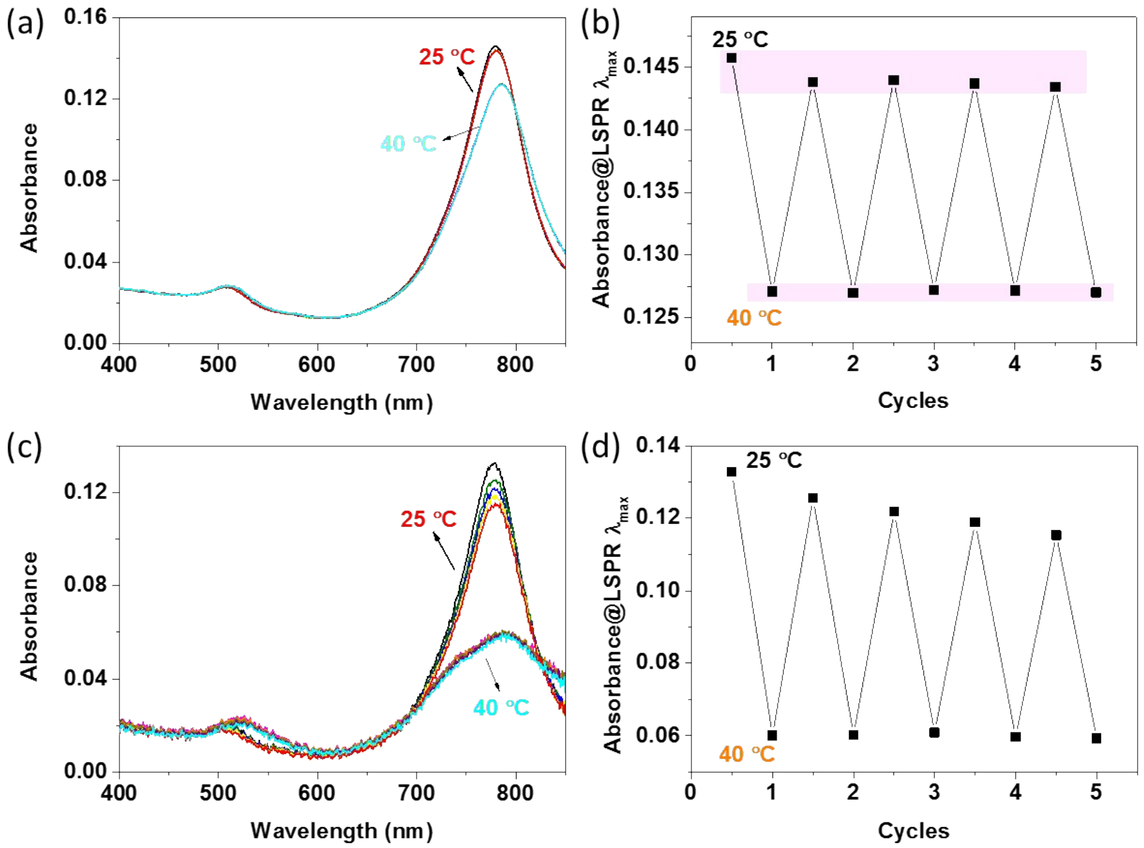

Figure S11. (a) Cycling test of NBP@PNIPAM between 25 to 40 °C in aqueous solution without NaCl. (b) Reversibility of the longitudinal mode peak intensity of NBP@PNIPAM as a function of the number of heating and cooling cycles in aqueous solution without NaCl. (c) Cycling test of NBP@PNIPAM with NaCl in the aqueous solution between 25 to 40 °C. (d) The longitudinal mode peak intensity of NBP@PNIPAM with NaCl in the aqueous solution as a function of the number of heating and cooling cycles.

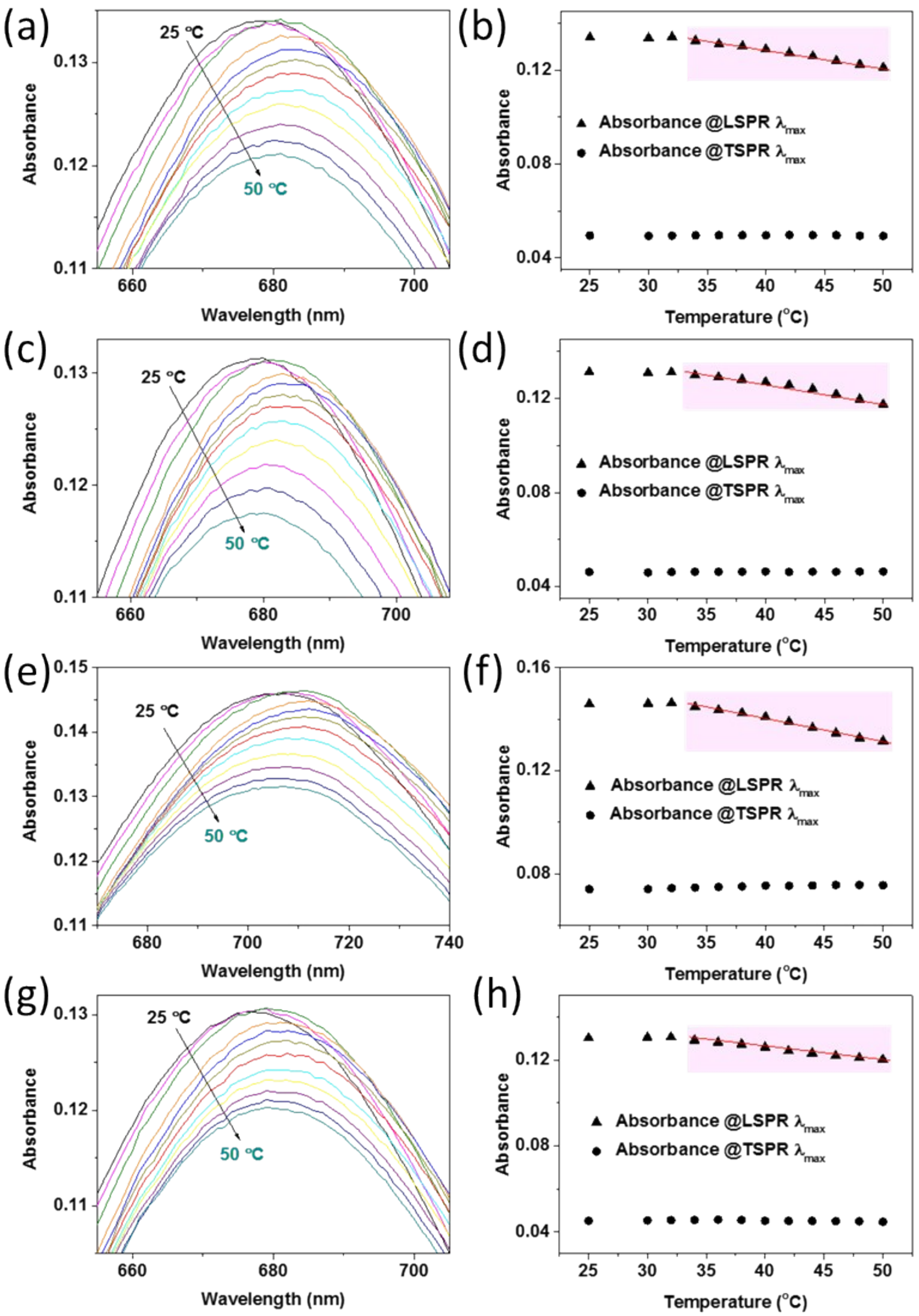

Figure S12. Linear correlations between longitudinal plasmonic peak intensities and solution temperatures of AuNR@PNIPAM across different batches.

References

1. Y. Chen, J. Fu, K. C. Ng, Y. Tang and W. L. Cheng, *Cryst. Growth Des.*, 2011, **11**, 4742-4746.
2. K. C. Ng, I. B. Udagedara, I. D. Rukhlenko, Y. Chen, Y. Tang, M. Premaratne and W. L. Cheng, *ACS Nano*, 2012, **6**, 925-934.
3. Q. Q. Shi, K. J. Si, D. Sikdar, L. W. Yap, M. Premaratne and W. L. Cheng, *ACS Nano*, 2016, **10**, 967-976.
4. Q. Li, X. L. Zhuo, S. Li, Q. F. Ruan, Q. H. Xu and J. F. Wang, *Adv. Opt. Mater.*, 2015, **3**, 801-812.
5. F. Han, A. H. Soeriyadi, S. R. C. Vivekchand and J. J. Gooding, *ACS Macro Lett.*, 2016, **5**, 626-630.
6. Q. Yan, J. Y. Yuan, W. Z. Yuan, M. Zhou, Y. W. Yin and C. Y. Pan, *Chem. Commun.*, 2008, 6188-6190.
7. J. He, Y. J. Liu, T. Babu, Z. J. Wei and Z. H. Nie, *J. Am. Chem. Soc.*, 2012, **134**, 11342-11345.
8. S. T. Jones, Z. Walsh-Korb, S. J. Barrow, S. L. Henderson, J. del Barrio and O. A. Scherman, *ACS Nano*, 2016, **10**, 3158-3165.
9. H. Petrova, J. P. Juste, I. Pastoriza-Santos, G. V. Hartland, L. M. Liz-Marzan and P. Mulvaney, *Phys. Chem. Chem. Phys.*, 2006, **8**, 814-821.
10. S. Mallawaarachchi, M. Premaratne, S. D. Gunapala and P. K. Maini, *Phys. Rev. B*, 2017, **95**, 155443.
11. G. Gerlach and K. J. Wolter, *Bio and nano packing techniques for electron devices: Advances in Electronic Device Packaging*, Berlin: Springer-Verlag, 2012.
12. S. Link, M. B. Mohamed and M. A. El-Sayed, *J. Phys. Chem. B*, 1999, **103**, 3073-3077.
13. S. Raza, S. I. Bozhevolnyi, M. Wubs and N. A. Mortensen, *J. Phys.-Condens. Mat.*, 2015, **27**, 183204.
14. K. Abdul-Kader, M. Lopes, C. Bartual-Murgui, O. Kraieva, E. M. Hernandez, L. Salmon, W. Nicolazzi, F. Carcenac, C. Thibault, G. Molnar and A. Bousseksou, *Nanoscale*, 2013, **5**, 5288-5293.
15. K. Kolwas and A. Derkachova, *Opto-Electron Rev.*, 2010, **18**, 429-437.
16. C. T. Kelley, *Solving nonlinear equations with Newton's method*, Society for Industrial and Applied Mathematics, 2003.